



| | |
|----------------------------------|---|
| Publication Year | 2017 |
| Acceptance in OA | 2020-08-31T07:21:12Z |
| Title | Multiple populations along the asymptotic giant branch of the globular cluster M4 |
| Authors | Lardo, C., Salaris, M., Savino, A., Donati, P., Stetson, P. B., CASSISI, Santi |
| Publisher's version (DOI) | 10.1093/mnras/stw3374 |
| Handle | http://hdl.handle.net/20.500.12386/26976 |
| Journal | MONTHLY NOTICES OF THE ROYAL ASTRONOMICAL SOCIETY |
| Volume | 466 |

Multiple populations along the asymptotic giant branch of the globular cluster M4

C. Lardo,^{1★} M. Salaris,¹ A. Savino,^{1,2} P. Donati,^{3,4} P. B. Stetson⁵ and S. Cassisi⁶

¹*Astrophysics Research Institute, Liverpool John Moores University, IC2, Liverpool Science Park, 146 Brownlow Hill, Liverpool L3 5RF, UK*

²*Kapteyn Astronomical Institute, University of Groningen, Postbus 800, NL-9700 AV Groningen, the Netherlands*

³*INAF – Osservatorio Astronomico di Bologna, via Ranzani 1, I-40127 Bologna, Italy*

⁴*Dipartimento di Fisica e Astronomia, via Ranzani 1, I-40127 Bologna, Italy*

⁵*Herzberg Astronomy and Astrophysics, National Research Council Canada, 5071 West Saanich Road, Victoria, BC V9E 2E7, Canada*

⁶*INAF – Osservatorio Astronomico di Teramo, Via M. Maggini, I-64100 Teramo, Italy*

Accepted 2016 December 21. Received 2016 December 21; in original form 2016 September 23

ABSTRACT

Nearly all Galactic globular clusters host stars that display characteristic abundance anticorrelations, like the O-rich/Na-poor pattern typical of field halo stars, together with O-poor/Na-rich additional components. A recent spectroscopic investigation questioned the presence of O-poor/Na-rich stars amongst a sample of asymptotic giant branch (AGB) stars in the cluster M4, at variance with the spectroscopic detection of a O-poor/Na-rich component along both the cluster red giant branch (RGB) and horizontal branch. This is contrary to what is expected from the cluster horizontal branch morphology and horizontal branch stellar evolution models. Here, we have investigated this issue by employing the $C_{UBI} = (U - B) - (B - I)$ index, that previous studies have demonstrated to be very effective in separating multiple populations along both the RGB and AGB sequences. We confirm previous results that the RGB is intrinsically broad in the $V-C_{UBI}$ diagram, with the presence of two components that nicely correspond to the two populations identified by high-resolution spectroscopy. We find that AGB stars are distributed over a wide range of C_{UBI} values, in close analogy with what is observed for the RGB, demonstrating that the AGB of M4 also hosts multiple stellar populations.

Key words: stars: abundances – stars: AGB and post-AGB – globular clusters: general – globular clusters: individual: M4.

1 INTRODUCTION

During the course of the last 15 yr, it has become increasingly well established that individual Galactic (and extragalactic) globular clusters host a stellar *first population* (FP) with initial chemical abundance ratios similar to the ones of field halo stars, plus additional sub-populations (that we collectively denote as second population – SP), each one characterized by its own specific variation of He (increased), C (decreased), N (increased), O (decreased), Na (increased) and sometimes Mg (decreased) and Al (increased) abundances (see e.g. Gratton, Carretta & Bragaglia 2012), compared to FP ratios. These abundance patterns give origin to well-defined (anti)correlations between pairs of light elements, the most characteristic ones being the Na–O and the C–N anticorrelations.

According to the currently most accepted scenarios, the observed abundance patterns are produced by high-temperature proton captures either at the bottom of the convective envelope of massive asymptotic giant branch (AGB) stars (see e.g. D’Ercole et al. 2008),

or in main-sequence (MS) fast rotating massive stars (Decressin et al. 2007), or supermassive stars (Denissenkov et al. 2015), belonging to the cluster FP. This chemically processed material is transported to the surface either by convection (in AGB stars and fully convective supermassive stars) or rotational mixing (in fast rotating massive stars), and spread in the intra-cluster medium by stellar winds. SP stars are supposed to have formed out of this gas, with a time delay that depends on the type of polluter, but it is always very short compared to the typical age of these old stellar systems.

In recent years, some controversy has arisen about the presence of SP stars along the AGB of some Galactic globular cluster (GGC). Standard stellar evolution (see e.g. Cassisi & Salaris 2013) dictates that horizontal branch (HB) stars with masses below $\sim 0.50\text{--}0.53 M_{\odot}$ (the exact value depending on the initial chemical composition) fail to reach the AGB phase (the so-called *AGB-manqué* stars, see Greggio & Renzini 1990), and SP stars are indeed expected to have on average a lower mass along the HB with respect to FP stars. In fact, given that SP stars are typically (to a more or lesser degree) He-enhanced, their HB progeny originate from the RGB stars with a lower mass compared to the FP RGB population,

★ E-mail: C.Lardo@ljmu.ac.uk

hence will be on average less massive (and bluer) than FP HB stars, if the RGB mass-loss is approximately the same for both FP and SP objects. The AGB of GGCs with a blue HB may therefore lack at least a fraction of SP stars, compared to what is seen along the RGB.

García-Hernández et al. (2015) found SP stars along the AGB of the GGCs M13, M5, M3 and M2, by combining the *H*-band Al abundances obtained by the Apache Point Observatory Galactic Evolution Experiment survey with ground-based optical photometry, although they did not study whether the SP/FP ratio was consistent with the corresponding ratio found on the RGB and the HB morphology.

The spectroscopic study by Campbell et al. (2013) found no SP stars along the AGB of NGC6752 (a cluster with a moderately extended blue HB), at odds with results from detailed synthetic HB modelling (Cassisi et al. 2014) showing that for the observed HB morphology, an SP component should be present along the AGB, that should lack only the more extreme Na-enhanced population. A later spectroscopic analysis by Lapenna et al. (2016) found AGB SP stars with moderate Na enhancement, as predicted by synthetic HB models.

Very recently MacLean et al. (2016) have found spectroscopically a lack of SP stars in M4. These authors claim that the AGB abundance distribution is consistent with all the AGB objects being FP stars, although their discussion mentions that due to the errors on [Na/Fe] and [O/Fe] abundance ratios, the presence of a few SP AGB stars cannot be excluded. This cluster has [Fe/H] ~ -1.1 (see e.g. Marino et al. 2011, and references therein) and an HB that does not extend above ~ 9000 K, hence it does not show any blue tail in the *BV* colour–magnitude diagram (CMD), and – as we will see in Section 3 – is populated by objects with masses above $0.55 M_{\odot}$. HB stellar models with the cluster chemical composition and this minimum mass do move to the AGB after core-He exhaustion. Moreover, the spectroscopic studies by Marino et al. (2011) and Villanova et al. (2012) have targeted some of the bluest HB stars in this cluster, and have measured Na abundances roughly as high as the highest Na abundances measured along the RGB (Marino et al. 2011, have also observed stars belonging to the red portion of the HB, that turned out to have typical FP composition). Given that these bluest Na-rich HB stars are expected to evolve on the AGB, a lack of SP stars along this phase is totally unexplainable by stellar evolution. Note that the bluest HB stars are cooler than the observed T_{eff} threshold for the onset of radiative levitation ($\sim 11\,000\text{--}12\,000$ K; see e.g. Grundahl et al. 1999; Behr 2003; Brown et al. 2016). This means that one cannot even consider the hypothesis by Campbell et al. (2013) – invoked to explain their results for NGC6752 – that enhanced HB mass-loss associated with the surface metal enhancement caused by radiative levitation that may push HB stars into the *AGB-manqué* regime (but see also Vink & Cassisi 2002, for a detailed investigation on this issue).

Given the uncertain claims of MacLean et al. (2016) paper, we revisit the issue of the AGB population in M4, using photometry. Recent observational and theoretical analyses have in fact shown how appropriate combinations of broad- and/or intermediate-band filters are capable to reveal the presence of multiple populations along the CMD branches of GGCs (see e.g. Marino et al. 2008; Yong et al. 2008; Sbordone et al. 2011; Milone et al. 2015b; Piotto et al. 2015, and references therein). Here, we make use of *UBVI* magnitudes, and the $C_{UBI} = (U - B) - (B - I)$ index (similar to the $(U - B + I)$ index by Milone et al. 2012b) that has been successfully employed to reveal the presence of multiple stellar populations along the AGB in a number of GCs (see e.g.

Milone et al. 2013; Monelli et al. 2013; García-Hernández et al. 2015; Milone et al. 2015a,b; Nardiello et al. 2015).

The next section describes briefly the photometric data, followed by an analysis of the cluster AGB and RGB using $V-C_{UBI}$ diagrams and conclusions.

2 PHOTOMETRIC DATA

Our optical observations of M4 are the same presented in Monelli et al. (2013) and Stetson et al. (2014). The Stetson et al. (2014) data set was further complemented with the observations listed in Table 1, for a grand total of 5351 individual CCD images obtained during the course of 25 observing runs. We refer to Stetson et al. (2014) for a description of the observational material.

All the CCD images were reduced and analysed by Peter B. Stetson using the DAOPHOT/ALLSTAR/ALLFRAME suite of programs. These data were then calibrated to the Johnson *UBV*, Kron/Cousins *RI* photometric system of Stetson (2000, 2005).¹ This analysis resulted in 80 480 stars in the M4 field with calibrated photometry in *V* and at least one of *B* or *I*; 79 146 stars had calibrated photometry in all three of *B*, *V* and *I*; and 31 791 of them had calibrated photometry in *U*, *B* and *I*. Further details on the reduction and analysis of the photometric material used in this paper can be found in Stetson et al. (2014).

Given the large value of $E(B - V)$ ($E(B - V) = 0.35\text{--}0.40$) and an anomalous large $R_V = A_V/E(B - V) \sim 3.8$ in the line of sight towards M4 (see e.g. Hendricks et al. 2012; Kaluzny et al. 2013, and references therein), we have corrected for the possible presence of differential reddening (DR) across the face of the cluster in the field of view of our observations. We followed the recipe described in Donati et al. (2014), that revises the method by Milone et al. (2012a). The reader is referred to the former paper for details. In brief, we have first considered MS stars in the $V - (B - V)$ CMD and drawn a reference fiducial line through the middle of the observed MS between $V = 17.5$ and 20.0 . For each star in the photometry, we then selected about 30 of the nearest (spatially) MS objects, and averaged their distance along the reddening vector direction from the MS ridge line in the CMD. This value was adopted as a DR correction for each star. Note that the mean value of the DR correction is not necessarily equal to zero, for it depends on the colour distribution of the MS stars around the adopted reference ridge line.

To correct the individual magnitudes for DR, we adopted $R_V = 3.8$ and $A_U = 1.43A_V$, $A_B = 1.22A_V$, $A_I = 0.62A_V$, as obtained by convolving the Cardelli, Clayton & Mathis (1989) reddening law with an ATLAS9 α -enhanced ([α /Fe] = 0.4) spectrum (Cassisi et al. 2004) for [Fe/H] = -1.0 , $\log(g) = 4.5$ and $T_{\text{eff}} = 5800$ K, corresponding to about 1 mag below the turn-off in *V* for a 12.5 Gyr isochrone with the same chemical composition (see Section 3).

We find that the total range of reddenings $\Delta E(B - V)$ spanned by 90 per cent of the cluster stars is equal to ~ 0.10 mag, consistent with the reddening map presented in Monelli et al. (2013).

A word of caution about the DR corrections determined in this fashion is in general necessary. According to the derivative $\Delta Y/\Delta(B - V) \sim 1$ for MS stars (obtained from Pietrinferni et al. 2006, models at varying *Y*), an *Y* range amongst the cluster sub-populations produces an intrinsic width of the MS, that could

¹ Please see <http://www1.cadc-ccda.hia-ihp.nrc-cnrc.gc.ca/community/STETSON/standards/>; see also <http://www.cadc.hia-ihp.nrc-cnrc.gc.ca/community/STETSON/homogeneous/archive/>

Table 1. Logs of observations in optical bands used in this paper, which complement the data set presented in Stetson et al. (2014)

| Run | ID | Dates | Telescope | Camera | <i>U</i> | <i>B</i> | <i>V</i> | <i>R</i> | <i>I</i> | Multiplex |
|-----------------|-----------|-------------------------|------------------|-------------------|----------|----------|----------|----------|----------|-----------|
| 19 ^a | wfi42 | 2000 April 1 | ESO/MPI 2.2 m | WFI | – | 3 | 4 | – | 4 | 8 |
| 20 ^b | wfi40 | 2007 July 9–13 | ESO/MPI 2.2 m | WFI | – | – | 10 | – | 11 | 8 |
| 21 ^c | Y1008 | 2010 August 14 and 15 | CTIO 1.0m | Y4KCam ITL SN3671 | – | 11 | 12 | – | – | – |
| 22 ^d | efosc1305 | 2013 May 14 and 15 | ESO NTT 3.6 m | EFOSC/1.57 LORAL | – | – | – | – | 14 | – |
| 23 ^e | lcogt4 | 2014 February 10 | Sutherland 1.0 m | CCD | – | – | 10 | – | 10 | – |
| 24 ^f | lcogt1 | 2014 March 27, April 10 | Sutherland 1.0 m | CCD | – | – | 18 | – | 9 | – |
| 25 ^g | efosc1406 | 2014 June 27 | ESO NTT 3.6 m | EFOSC/1.57 LORAL | – | – | 13 | – | 9 | – |

Notes. The column ‘multiplex’ refers to the number of individual CCD chips in the particular camera, which were treated as independent detectors. ^aESO Program ID 164.O–0561(F); ^bESO Program ID 079.D–0918(A); ^cSMARTS Project ID Sejong10B; ^dESO Program ID 091.D–0711(A); ^eProposal ID STANET–002; ^fProposal ID STANET–002; and ^gESO Program ID 093.D–0264(A).

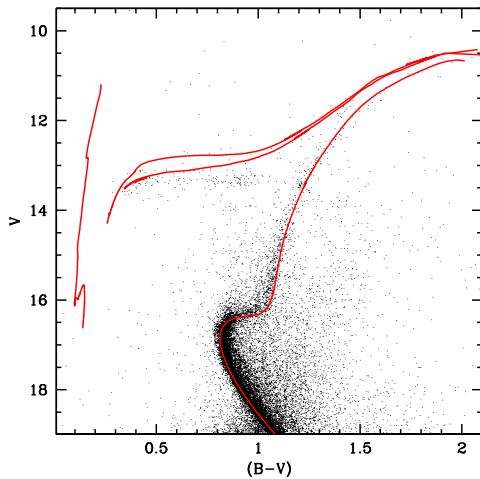


Figure 1. Comparison of a 12.5 Gyr isochrone with $[\text{Fe}/\text{H}] = -1.0$ and $[\alpha/\text{Fe}] = 0.40$, with the cluster $V - (B - V)$ CMD. We display also HB evolutionary tracks for masses equal to (from the red to the blue) 0.58 , 0.56 and $0.495 M_{\odot}$, respectively. A distance modulus $(m - M)_0 = 11.30$ and reddening $E(B - V) = 0.34$ ($R_V = 3.8$ – see text for details) have been employed.

potentially cause an overestimate of the range spanned by $E(B - V)$. This potential systematic error will depend on the range of ΔY , and the relative fraction of the FP and SP MS stars employed to determine the DR correction for each object in the photometry.

As pointed out by our referee, this is however not a matter of concern for M4. Determinations of ΔY in the literature range from negligible values (Valcarce et al. 2014), up to just ~ 0.02 (Villanova et al. 2012; Nardiello et al. 2015). The fraction of SP stars in this cluster is approximately the same between the central (Milone et al. 2016) and external (Marino et al. 2008; Nardiello et al. 2015) regions analysed so far, being equal to 30–40 per cent; this fraction, together with a maximum $\Delta Y = 0.02$ would cause systematic effects on the reddening below 0.01 mag.

3 ANALYSIS

Before starting the analysis of M4 $V - C_{UBI}$ diagram, we display in Fig. 1 the $V - (B - V)$ CMD corrected for DR, compared to theoretical isochrones. We employ here BaSTI (Pietrinferni et al. 2006) α -enhanced isochrones² with $[\text{Fe}/\text{H}] = -1.01$ ($[\alpha/\text{Fe}] = 0.4$), He mass fraction $Y = 0.251$, a distance modulus $(m - M)_0 = 11.30$ as

obtained by Kaluzny et al. (2013) from the analysis of three cluster eclipsing binaries, $E(B - V) = 0.34$ and $R_V = 3.8$. Note that in the BV CMD theoretical isochrones with a standard α -enhanced metal mixture (employed in both the stellar model and stellar spectra calculations) are appropriate to match also SP stars (see Sbordone et al. 2011; Cassisi et al. 2013). Also, the range of He abundance (expressed as mass fraction Y) estimated for the cluster populations is very small, with ΔY equal to 0.02 or less (Villanova et al. 2012; Valcarce et al. 2014; Nardiello et al. 2015).

The purpose of this comparison – that is not meant to be a perfect fit model-theory – is to show very clearly how HB stellar models predict that all HB stars in this cluster evolve to the AGB phase. The mass of the HB track that starts the evolution at the hottest end of the observed HB is equal to approximately $0.58 M_{\odot}$. Observationally the onset of radiative levitation is at $\sim 12\,000$ K, corresponding to the zero-age HB location of the $0.56 M_{\odot}$ track shown in the figure. Note how this threshold (in the hypothesis it could trigger a very strong wind that decreases rapidly the stellar mass) is well beyond the hot end of the observed HB. We also display, just for the sake of comparison, the most massive ($M = 0.495 M_{\odot}$) AGB-*manqué* star.

As shown by Marino et al. (2008) and Sbordone et al. (2011) the $(U - B)$ colour is very sensitive to light-element variations, whereas the $(B - I)$ colour is unaffected and is mainly sensitive to T_{eff} variations. The combination $C_{UBI} = (U - B) - (B - I)$ is therefore able to segregate FP and SP stars in a $V - C_{UBI}$ diagram as discussed in Milone et al. (2013), Monelli et al. (2013) and García-Hernández et al. (2015), producing either multimodal or very broad sequences, broader than expected from the photometric error. This is true also for AGB stars, as shown empirically by García-Hernández et al. (2015), Monelli et al. (2013), Milone et al. (2015a,b) and Nardiello et al. (2015).

To look for signatures of SP stars along M4 AGB stars in the $V - C_{UBI}$ plane, we follow a standard procedure similar to the one outlined in Monelli et al. (2013). We first cleaned the CMD from foreground/background contamination, i.e. cluster membership has been assigned on the basis of the source position in the $(B - I)$ versus $(U - V)$ plane (see fig. 2 in Monelli et al. 2013). As a first step, we defined AGBs as shown in the top-left panel of Fig. 2. Then, we plotted the selected stars in other CMDs that provide the cleanest separation of the evolved sequences to help verify the identification (see Fig. 2). To this aim, we cross-correlated our $UBVI$ photometry with the 2MASS catalogue³ to carefully inspect the position of selected AGB stars in CMDs including near-infrared colours. All selected stars are compatible with being AGBs in all diagrams displayed in Fig. 2. This demonstrates that they cannot be RGBs

² <http://www.oateramo.inaf.it/BASTI>

³ <http://www.ipac.caltech.edu/2mass/>

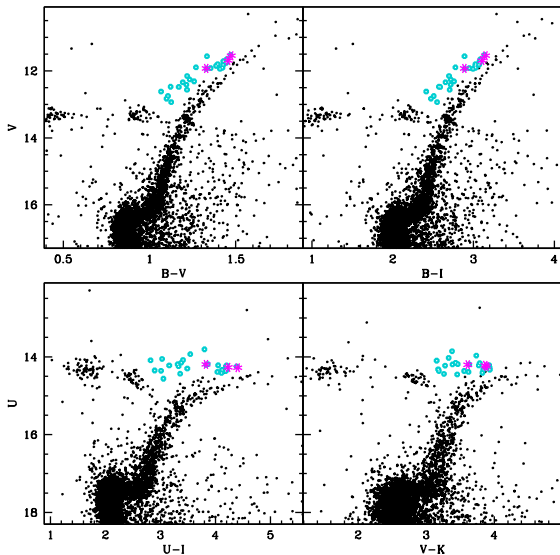


Figure 2. Selection of AGB star candidates in different CMDs. From top-to-bottom: $V, B - V$; $V, B - I$; and $U, U - I$. Empty cyan symbols are AGB stars. Magenta asterisks mark candidate AGB stars in common with Marino et al. (2008).

migrated to the AGB sequence due to photometric errors. Indeed, no random errors can explain that the selected stars are always located in a well-defined sequence bluer of the main body of the RGB in different CMDs obtained from independent measurements/data sets. From all the above, we conclude that the selected stars are indeed AGBs. We finally note that the observed AGB/RGB ratio ($R_{\text{AGB/RGB}} = 0.44 \pm 0.23$) agrees within the errors with the theoretical one ($R_{\text{AGB/RGB}} = 0.37$). This by itself is obviously not a proof that all candidate AGBs are indeed AGB stars, but just a consistency check for our empirically derived value of $R_{\text{AGB/RGB}}$.

To assess whether some significant residual contamination may still be present in our AGB sample after the field-star subtraction, we used the code TRILEGAL (Girardi et al. 2005). We determined the fraction of Galactic field stars within a box $\simeq 30 \times 30$ arcmin² (i.e. comparable to the FoV of our photometric catalogue) centred on the cluster centre that survive our cluster AGB selection. We found one star with colours and magnitudes consistent with being on the cluster AGB, to be compared with the two AGB objects rejected with our field-subtraction procedure. This implies that any residual field contamination is very likely negligible.

Fig. 3 shows the $V-C_{\text{UBI}}$ diagram, with AGB stars highlighted. As already shown by Monelli et al. (2013), the RGB shows a large C_{UBI} spread at fixed V , that exceeds the spread due to photometric errors, and a hint of bimodality can also be observed.

Detailed $[\text{Na}/\text{Fe}]$ and $[\text{O}/\text{Fe}]$ abundances do exist for a number of bright RGB stars in this cluster (e.g. Marino et al. 2008; Carretta et al. 2009), and in the inset of Fig. 3, we show the NaO anticorrelation measured by Marino et al. (2008). The distribution of RGB stars in the $[\text{Na}/\text{Fe}]-[\text{O}/\text{Fe}]$ plane is clearly bimodal, with FP stars being clustered around $[\text{Na}/\text{Fe}] \simeq 0.1$ and $[\text{O}/\text{Fe}] \simeq 0.5$ dex. Conversely SP stars show enhanced Na abundances and are depleted in their O content. FP and SP stars – as defined by spectroscopy – appear clearly segregated along two parallel sequences in the $V-C_{\text{UBI}}$ diagram (see Fig. 3). This shows how the C_{UBI} index is very effective in separating the different stellar populations hosted in M4 (Monelli et al. 2013). AGB stars at a given V span a very similar

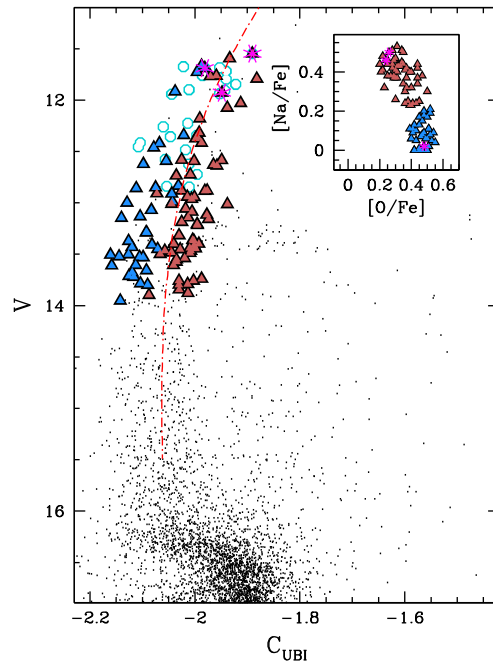


Figure 3. $V-C_{\text{UBI}}$ diagram is shown. AGB stars and stars in common with the Marino et al. (2008) study are marked with the same symbols as in Fig. 2. We display also a fiducial reference line (dash-dotted line) employed to quantify the broadening of the RGB and AGB sequences (see text for details). This line is just for reference, and is not meant to separate in this plot the location of FP and SP stars. The inset shows the NaO anticorrelation found by Marino et al. (2008) in M4 RGB stars. FP and SP stars are plotted as blue and red triangles, respectively, in the $V-\Delta C_{\text{UBI}}$ plane.

C_{UBI} range as RGB stars, suggesting that multiple stellar population are present also along the AGB stage.

A reference fiducial line in the $V-C_{\text{UBI}}$ diagram (shown Fig. 3) has been used to verticalize the $V-\Delta C_{\text{UBI}}$ diagram and quantify the spread of both AGB and RGB sequences. ΔC_{UBI} differences have been derived by subtracting from the C_{UBI} index of each star the corresponding value of the fiducial at the same V magnitude (e.g. Lardo et al. 2011), and the resulting diagram is shown in the top panel of Fig. 4, where spectroscopic FP and SP RGB stars, and AGB stars are marked. The lower panels of Fig. 4 display the number distributions of RGB and AGB ΔC_{UBI} values in three V -magnitude ranges. We find that AGB stars span the same total ΔC_{UBI} range as the RGB ones in the common magnitude range ($11 < V \leq 13$), and share the same 1σ spread (0.04 mag). We adopt the bootstrapped σ as the uncertainty on our estimate of the observed spread and find that the spread in colour in ΔC_{UBI} has standard deviation equal to 0.040 ± 0.005 and 0.041 ± 0.005 for AGBs and RGBs in the magnitude range $11 < V \leq 13$ mag, respectively. We also determined with a Kolmogorov–Smirnov (KS) test that the probability, we can reject that hypothesis that the observed ΔC_{UBI} distributions of AGB and RGB stars ($11 < V \leq 13$) are the same, is well below the standard 95 per cent threshold (it is equal to just 50 per cent). Finally, we performed a KS test on the distribution of the bootstrapped estimates of both the mean (ΔC_{UBI}) and the dispersion of ΔC_{UBI} for the distributions of AGB and blue and red RGB stars brighter than $V = 13$ mag. We find that both the mean and the dispersion of ΔC_{UBI} for AGB and (blue+red) RGB stars are compatible with being the same, while the same statistical test shows that the mean and the dispersion of ΔC_{UBI} for AGB, blue RGB and red RGB star groups (where the blue and red RGB stars

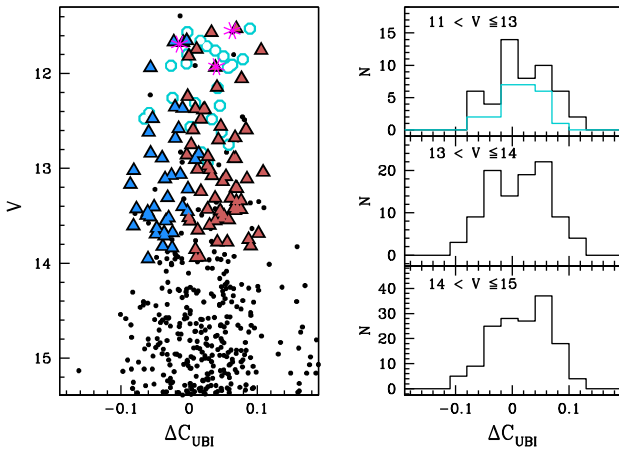


Figure 4. Verticalized $V-\Delta C_{UBI}$ diagram for bright giant stars (see text for details). The number distribution of AGB (cyan histogram) and RGB (black histogram). ΔC_{UBI} index differences with respect to the RGB fiducial in three V -magnitude bins are also shown. Magenta asterisks mark candidate AGB stars in common with Marino et al. (2008).

are taken into account separately) cannot be extracted from the same parent distribution. This leads us to conclude that the distribution in colours of AGB and RGB stars in the C_{UBI} index are statistically indistinguishable.

The demonstrated ability of the C_{UBI} index to separate FP and SP stars along both RGB and AGB (e.g. Monelli et al. 2013; García-Hernández et al. 2015; Milone et al. 2015a,b; Nardiello et al. 2015), plus the broad and consistent distribution of C_{UBI} covered by both RGB (where the presence of FP and SP stars is established spectroscopically) and AGB stars make a compelling case for the presence of SP stars also along the AGB of M4. These conclusions do not depend on the DR correction we performed, as we recovered the same result using as input catalogue the M4 photometry where DR variations have not been taken into account.

Also, Figs 3 and 4 show three of the stars observed by Marino et al. (2008) that should be classified as AGB rather than RGB stars according to their CMD location, as shown in Fig. 2. Based on their Na abundances, two of them are SP stars, while the remaining one has both [Na/Fe] and [O/Fe] abundances as the field at the same metallicity (see inset in Fig. 3). This further demonstrates that multiple population can be found also among AGB stars.

4 CONCLUSIONS

We have presented a multiwavelength photometric analysis of the RGB and AGB stars in the GGC M4, to establish whether SP stars are present along the cluster AGB sequence, as expected from the observed HB morphology, results from HB star spectroscopy and stellar evolution calculations. The analysis of the C_{UBI} index distribution of AGB and RGB stars provides compelling evidence for the presence of SP stars also along the cluster AGB (see Figs 3 and 4). Indeed, the presence of multiple stellar populations along the AGB, has been already detected photometrically in several GCs, using a similar approach as the one adopted here (e.g. Monelli et al. 2013; Milone et al. 2015a,b; Nardiello et al. 2015).

We also show that three stars analysed in Marino et al. (2008) should be classified as candidate AGB rather than RGB stars according to their position in the CMD. Such stars display a spread in [Na/Fe] ~ 0.45 dex; i.e. they belong to different populations.

Our result is in apparent contrast with what found by MacLean et al. (2016) spectroscopic study. An investigation of the reasons of this discrepancy is beyond the purposes of this study. However, we note that those authors admittedly expressed, some caution about their results, i.e. their uncertainties in Na and O abundances did not allow us to draw firm conclusions on the complete absence of SP stars in M4 AGB.

None the less, blue HB stars with the highest Na enrichment have the same maximum Na enrichment displayed by RGB stars (Marino et al. 2011; Villanova et al. 2012) and are expected to evolve to the AGB according to standard stellar evolution. Hence, the photometric discovery of SP stars in the AGB of M4 well fits within the standard stellar evolution framework.

ACKNOWLEDGEMENTS

We thank the anonymous referee for a detailed report that helped to improve the presentation of our results. CL gratefully acknowledges financial support from the European Research Council (ERC-CoG-646928, Multi-Pop, PI: N. Bastian). SC acknowledges the financial support by PRIN-INAF2014 (PI: S. Cassisi).

REFERENCES

- Behr B. B., 2003, *ApJS*, 149, 67
 Brown T. M. et al., 2016, *ApJ*, 822, 44
 Campbell S. W. et al., 2013, *Nature*, 498, 198
 Cardelli J. A., Clayton G. C., Mathis J. S., 1989, *ApJ*, 345, 245
 Carretta E. et al., 2009, *A&A*, 505, 117
 Cassisi S., Salaris M., 2013, *Old Stellar Populations: How to Study the Fossil Record of Galaxy Formation*. Gordon and Breach, New York
 Cassisi S., Salaris M., Castelli F., Pietrinferni A., 2004, *ApJ*, 616, 498
 Cassisi S., Mucciarelli A., Pietrinferni A., Salaris M., Ferguson J., 2013, *A&A*, 554, A19
 Cassisi S., Salaris M., Pietrinferni A., Vink J. S., Monelli M., 2014, *A&A*, 571, A81
 D’Ercole A., Vesperini E., D’Antona F., McMillan S. L. W., Recchi S., 2008, *MNRAS*, 391, 825
 Decressin T., Meynet G., Charbonnel C., Prantzos N., Ekström S., 2007, *A&A*, 464, 1029
 Denissenkov P. A., VandenBerg D. A., Hartwick F. D. A., Herwig F., Weiss A., Paxton B., 2015, *MNRAS*, 448, 3314
 Donati P., Beccari G., Bragaglia A., Cignoni M., Tosi M., 2014, *MNRAS*, 437, 1241
 García-Hernández D. A., Mészáros S., Monelli M., Cassisi S., Stetson P. B., Zamora O., Shetrone M., Lucatello S., 2015, *ApJ*, 815, L4
 Girardi L., Groenewegen M. A. T., Hatziminaoglou E., da Costa L., 2005, *A&A*, 436, 895
 Gratton R. G., Carretta E., Bragaglia A., 2012, *A&AR*, 20, 50
 Greggio L., Renzini A., 1990, *ApJ*, 364, 35
 Grundahl F., Catelan M., Landsman W. B., Stetson P. B., Andersen M. I., 1999, *ApJ*, 524, 242
 Hendricks B., Stetson P. B., VandenBerg D. A., Dall’Ora M., 2012, *AJ*, 144, 25
 Kaluzny J. et al., 2013, *AJ*, 145, 43
 Lapenna E. et al., 2016, *ApJ*, 826, L1
 Lardo C., Bellazzini M., Pancino E., Carretta E., Bragaglia A., Dalessandro E., 2011, *A&A*, 525, A114
 MacLean B. T., Campbell S. W., De Silva G. M., Lattanzio J., D’Orazi V., Simpson J. D., Momany Y., 2016, *MNRAS*, 460, L69
 Marino A. F., Villanova S., Piotto G., Milone A. P., Momany Y., Bedin L. R., Medling A. M., 2008, *A&A*, 490, 625
 Marino A. F., Villanova S., Milone A. P., Piotto G., Lind K., Geisler D., Stetson P. B., 2011, *ApJ*, 730, L16
 Milone A. P. et al., 2012a, *A&A*, 540, A16

- Milone A. P. et al., 2012b, *ApJ*, 744, 58
Milone A. P. et al., 2013, *ApJ*, 767, 120
Milone A. P. et al., 2015a, *MNRAS*, 447, 927
Milone A. P. et al., 2015b, *ApJ*, 808, 51
Milone A. P. et al., 2016, *MNRAS*, 455, 3009
Monelli M. et al., 2013, *MNRAS*, 431, 2126
Nardiello D., Milone A. P., Piotto G., Marino A. F., Bellini A., Cassisi S., 2015, *A&A*, 573, A70
Pietrinferni A., Cassisi S., Salaris M., Castelli F., 2006, *ApJ*, 642, 797
Piotto G. et al., 2015, *AJ*, 149, 91
Sbordone L., Salaris M., Weiss A., Cassisi S., 2011, *A&A*, 534, A9
Stetson P. B., 2000, *PASP*, 112, 925
Stetson P. B., 2005, *PASP*, 117, 563
Stetson P. B. et al., 2014, *PASP*, 126, 521
Valcarce A. A. R., Catelan M., Alonso-García J., Cortés C., De Medeiros J. R., 2014, *ApJ*, 782, 85
Villanova S., Geisler D., Piotto G., Gratton R. G., 2012, *ApJ*, 748, 62
Vink J. S., Cassisi S., 2002, *A&A*, 392, 553
Yong D., Grundahl F., Johnson J. A., Asplund M., 2008, *ApJ*, 684, 1159

This paper has been typeset from a $\text{\TeX}/\text{\LaTeX}$ file prepared by the author.